Electronic Structure of Substitutional 3d Impurities in $\gamma' - Fe_4N$

J. C. Krause[a] and C. Paduani[b]

[a] *Instituto de Física, Universidade Federal do Rio Grande do Sul, UFRGS, Porto Alegre, CEP 91501-970, RS, Brazil*

[b] *Departamento de Física, Universidade Federal de Santa Catarina, UFSC, Florianópolis, CEP 88040-900, SC, Brazil*

Received October 4, 1995

The magnetic and electronic structure of 3d localized impurities (Sc, Ti, V, Cr, Mn, Co, Ni, Cu and Zn) in the ferromagnetic iron nitride $\gamma' - Fe_4N$ are investigated in molecular cluster calculations with the discrete variational (DV) method. The calculations rely on the local spin density approximation of the density functional theory. The cluster is embedded in the long-ranged Coulombian crystal field potential, consisting of 300 atoms. The magnetic moment (μ), hyperfine magnetic field (H_c), density of states (DOS) and charge transfer are obtained for the central atom of each cluster. The results indicate that, at corner iron sites (named FeI), all these atoms behave as magnetic impurities, being that the Mn, Cr and Co atoms exhibit the largest μ value. At face centered iron sites (named FeII), except for Cu, all the others atoms are magnetic impurities, with the largest μ values belonging to the Mn, V and Co impurities. At both FeI and FeII sites the Mn atom has the largest H_c value. The N atom still acts as an acceptor for electrons, at both nonequivalent iron sites.

I. Introduction

Among the promising candidates for technological applications in magnetic recording devices, the magnetic nitrides have attracted special attention since few decades ago. In this class, the ferromagnetic iron nitride $\gamma' - Fe_4N$ has been intensively investigated in recent years, by several theoretical studies and a large variety of experimental techniques[1-6]. In particular, one interesting feature that has attracted attention, is the behavior of the N atom with respect to the charge transfer in this matrix. Several papers have been published discussing this point, and indeed, there is a general consensus that N behaves as an acceptor for electrons[4, 5, 6].

This compound has a simple cubic crystal structure, composed of fcc iron, with the nitrogen atom at the body center site. In order to improve both magnetic and mechanical properties, a large number of experimental studies have been realized, searching for good candidates to substitute the iron atoms in this nitride. Among others, Ni, Pd, Pt have been used as a third component in this host[7, 8, 9].

Cluster calculations have been applied to investigate the electronic structure of dilute magnetic impurities in noble metals by Delley *et al.*[10]. The results are in good agreement with the Green function KKR method, and could even describe experimental results. The authors claim that no discrepancy exists between cluster and continuous models, if one chooses clusters of a suitable size. The first-principles DV molecular cluster method have been successfully applied to investigate several metallic systems[11-14]. In this work is investigated the formation of localized magnetic states at impurities atoms in $\gamma' - Fe_4N$ host, for the 3d series of the iron group atoms. The calculations are performed in spin-polarized case, with the DV method, which is

described in detail elsewhere in the literature[15]. These calculations have been carried out along the same procedure described in [6], and so in the next sections we will restrict the presentation to our results.

II. Details of calculations

The molecular cluster DV method is a numerical-variational method which employs the Hartree-Fock-Slater model. Is employed in these calculations with the exchange-correlation potential of Barth-Hedin, of the density functional theory[17]. The crystal is approximated by a cluster consisting of few shells of neighbors around the central atom. In order to build up the molecular orbitals, it is used a a linear combination of atomic orbitals (MO-LCAO), where the atomic basis is generated by solving the self-consistent atom problem. The matrix elements of the Hamiltonian and overlap are evaluated by direct numerical integration procedures, using a random sampling method, where a sum of Fermi-type functions around each atom is adopted as the distribution function of the sample points[16].

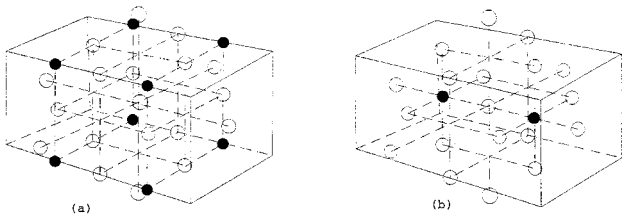

Figure 1. (a) Cluster of 27 atoms representing the first and second neighborhoods of a FeI site : $FeI(FeII)_{12}N_8(FeI)_6$; the full circles indicate N atoms. (b) the cluster with 21 atoms, for a FeII site : $FeII(N)_2(FeII)_4(FeI)_8(FeII)_6$. The origin is in the central atom of each cluster.

The calculations were performed on two types of clusters. The first type contains 21 atoms, representing the first and second shell of neighbors of an iron atom around a FeII site and a N site. The second one includes 27 atoms, representing the immediate neighborhood of a FeI site in this matrix. Both are shown in Fig. 1. The experimental value of 7.1754 a.u. was adopted for the lattice spacing.

The minimal basis was used to build up the molecular orbitals, which includes 1s to 4p orbitals for the $3d$ atoms, and 1s to 3s, for N atoms. For the Zn atom the 5s orbital was added. In order to perform the numerical integration, about 250 points per atom were distributed in the cluster region. The cluster is embedded in the crystal potential, consisting of about 300 atoms. The potential wells, located at outer atoms in the crystal region, were truncated at the Fermi energy, to prevent an outflow of electrons towards low-lying states located on crystal atoms. The external potential floor was set up at the Fermi energy. A detailed description of the embedding scheme can be found in the literature[10, 18, 19]. After each cycle, a Mulliken population analysis of the molecular eigenfunctions is performed, in order to generate the atomic populations.

The central atom of each cluster is the probe atom, which has bulk-like properties. The truncation of the cluster does not allow sufficient wavefunction delocalization to take place, and so, the local magnetic moments tend to be more atomic-like [11]. Thus, a finite cluster effect is that, departing from the central atom toward the surface of the cluster, it is observed increasing values for the magnetic moments. Actually, only the central atom of each cluster, which is in the origin of the coordinate system, has the closest environment to the crystaline ambient, and is the more adequate probe to give reliable results for the bulk properties.

III. Results and Discussion

Table 1 summarizes calculated results at the FeI site, for the atomic populations $(s + p)$ and d, total magnetic moment (μ) besides the contribution from the conduction band 4s+4p to the total magnetic moment (μ_c), H_c and ionization (Q) for the central atom of each cluster, together with these values for their immediate neighborhood.

Table 1. Electronic populations $(s+p)$ and d, total magnetic moment (μ), the contribution to the local magnetic moment from the conduction band 4s+4p (μ_c), ionization (Q) and hyperfine magnetic field (H_c) values for the central atom at FeI site. The values of Q_N and μ_N stands for the nitrogen site. Also are included those values for the iron sites at the first (NN) and second (NNN) neighborhood.

Impurity	Sc	Ti	V	Cr	Mn	Fe	Co	Ni	Cu	Zn
$s+p$	0.9409	1.1205	1.2424	1.2798	1.3223	1.3769	1.4542	1.7307	1.8884	2.0749
d	1.6542	3.4407	3.4407	4.4476	5.4882	6.4844	7.3977	7.9759	8.9387	9.8517
Q	0.52	0.46	0.38	0.31	0.23	0.17	0.17	0.24	0.22	0.04
μ	-0.65	-1.07	-1.63	0.82	1.80	2.03	1.26	0.72	-0.01	-0.31
μ_c	-0.23	-0.27	-0.30	0.05	-0.17	-0.17	0.20	-0.17	0.18	-0.22
H_c	-285	-265	-223	-301	-536	-267	-517	-301	0	93
Q_N	-0.21	-0.20	-0.19	-0.17	-0.17	-0.17	-0.17	-0.16	-0.16	-0.15
μ_N	-0.20	-0.19	-0.16	-0.24	-0.25	-0.26	-0.24	-0.22	-0.21	-0.22
$(s+p)_{NN}$	1.5483	1.5449	1.5417	1.5499	1.5442	1.5424	1.5422	1.5463	1.5420	1.5255
d_{NN}	6.4687	6.4678	6.4654	6.4458	6.4551	6.4528	6.4531	6.4558	6.4575	6.4591
μ_{NN}	2.37	2.36	2.37	-2.51	2.48	2.52	2.52	2.51	2.49	2.45
$\mu_{c_{NN}}$	-0.01	-0.01	0.00	-0.02	0.02	-0.03	0.02	0.02	0.02	0.01
$(s+p)_{NNN}$	1.7508	1.7492	1.7462	1.7924	1.7466	1.7433	1.7473	1.7502	1.7489	1.7292
d_{NNN}	6.4193	6.4166	6.4122	6.3723	6.3995	6.3959	6.3953	6.3994	6.3991	6.4002
μ_{NNN}	3.13	3.12	3.13	3.53	3.24	3.27	3.28	3.27	3.27	3.25
$\mu_{c_{NNN}}$	0.05	0.06	0.07	0.40	0.08	0.07	0.08	0.09	0.09	0.08

Note in table 1 how the ionization decreases rapidly, from Sc down to Cr, which remains almost neutral at this site. Above $Z = 25$ the impurities atoms behave as atractors for electrons, whereas Mn, Ni and Cu atoms are well screened. The Zn atom enters as a positive charge in this host, with its tiny magnetization coming up entirely from the conduction electrons. The impurity magnetic moment (μ) increases steadly from Sc up to Mn, which exhibits the highest value, as normally occurs in this series. All of these elements display an opposite orientation of $\vec{\mu}$, relative to iron sites. One can observe the small contribution from the conduction band μ_c to the total magnetic moment at the impurity site. Actually, it is practically absent for iron. In proceeding further, Co, Ni and Cu have $\vec{\mu}$ aligned parallel to the iron sites. The contribution μ_c follows the same behavior of μ, from Sc to Mn, with an abrupt decrease thereafter.

The H_c value corresponds to the Fermi contact term in this case, considering that the orbital and dipolar contributions are vanishingly small for these atoms. The calculation was done in the same way as described in refs. [6,11]. The H_c value also follows the same behavior of μ, reaching a maximum at the Mn atom, where it changes signal. Except for Fe, Co, Ni and Cu, it has a positive value in this series, with the lowest value for the Cu atom. Observe that the signal of H_c is reversed at the same time as it occurs for μ. These results indicate that a linear correlation indeed exists

between H_c and the magnetization.

The ionization of the N atom (Q_N) is independent of the occupancy of the central site, and indicates an acceptor character for electrons at this site, which has a practically constant inflow of electrons coming up mainly from FeII sites. The μ values at N sites are small, and increase slightly by increasing the impurity atomic number, staying aligned antiparallel to the iron sites, reaching a maximum for the Co central atom.

The 12 iron atoms at FeII sites are the first neighbors of the impurity located at FeI sites, whose μ_{NN} values are also shown in table 1. A noticeable feature from the table is the complete depolarization of the conduction band, for these first neighbors, in spite of the fact that the magnetic polarization of d electrons follows the impurity behavior for the absolute value of μ. Moreover, with the introduction of the impurities atoms in this host the number of conduction electrons of the iron atoms at the first neighborhood $(s+p)_{NN}$ is increased. The addition of these impurities in this host decreases the magnetic polarization of the iron atoms at the first neighborhood (μ_{NN}), for those atoms which are at the left of Fe in the periodic table. Otherwise, for the other ones is observed enhanced μ values.

Furthermore, the iron atoms at the second neighborhood at FeI sites were almost insensitive to the number of d electrons at the impurity site, as one can verify in the table.

Table 2. The calculated results for the FeII sites, similarly as those showed in table 1 for FeI sites.

Impurity	Sc	Ti	V	Cr	Mn	Fe	Co	Ni	Cu	Zn
$s+p$	1.0366	1.2878	1.4655	1.5633	1.6659	1.5766	1.7118	2.0335	2.0447	2.3446
d	1.7064	2.5244	3.4417	4.4195	5.3985	6.5042	7.4652	7.9579	8.9334	9.9149
Q	0.30	0.21	0.11	0.03	-0.05	-0.07	-0.17	-0.04	-0.06	-0.29
μ	-0.36	-0.72	-1.36	-2.40	-3.38	2.99	2.11	1.59	0.54	-0.18
μ_c	-0.09	-0.13	-0.18	-0.25	-0.31	-0.01	-0.06	-0.08	-0.14	-0.18
H_c	62	87	137	244	349	-333	-215	-138	-14	104
Q_N	-0.41	-0.41	-0.41	-0.42	-0.42	-0.42	-0.42	-0.41	-0.42	-0.43
μ_N	-0.05	-0.09	-0.09	-0.10	-0.11	-0.12	-0.14	-0.13	-0.13	-0.12
$(s+p)_{NN}$	1.4087	1.4026	1.3983	1.3891	1.3809	1.3647	1.3722	1.3824	1.3798	1.3451
d_{NN}	6.4437	6.4401	6.9887	6.4311	6.4430	6.4314	6.4265	6.4305	6.4276	6.4347
μ_{NN}	0.85	0.90	1.03	1.09	1.10	1.33	1.43	1.40	1.39	1.28
μ_{cNN}	-0.03	-0.03	-0.02	-0.01	0.00	-0.02	0.00	0.01	0.00	-0.01
$(s+p)_{NNN}$	1.3949	1.3959	1.3783	1.4000	1.4042	1.4534	1.4039	1.4008	1.4031	1.4168
d_{NNN}	6.4455	6.4469	6.4574	6.4481	6.4482	6.4198	6.4502	6.4509	6.4546	6.4459
μ_{NNN}	3.59	3.58	3.52	3.55	3.5566	3.64	3.55	3.55	3.54	3.56
μ_{cNNN}	0.24	0.23	0.20	0.21	0.21	0.24	0.21	0.20	0.20	0.21

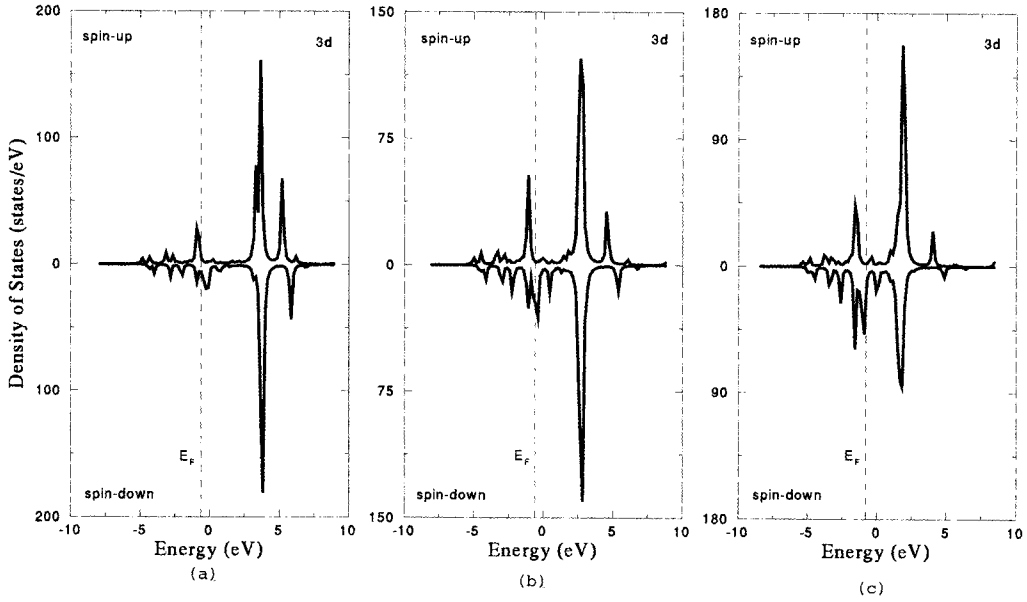

Figure 2. 3d PDOS for the Sc (a), Ti (b) and V (c) impurities at the FeI site. The upper part of the diagram indicates spin-up states and the lower part the spin-down states. The vertical line indicates the Fermi level.

Table 2 presents the calculated results for the impurities located at FeII sites. Note the decreasing (positive) ionization (Q value) from Sc down to Co, and further, the neutral behavior of the Zinc atom in this site, contrary to the high negative ionization at FeI site. The Sc atom exhibits the largest Q value. At these sites μ increases from Sc up to Mn (where it is maximum) decreasing further towards the total collapse for the Cu atom. The Zn atom shows a small μ value. Except for Sc, Ti, V and Zn all impurities have $\vec{\mu}$ parallel to that of the first neighborhood. The μ_c contribution is always negative throughout this series, with the smallest value for chromium.

In this case H_c do not follow the μ behavior, although displaying the highest value for the Mn atom. A remarkable result is the zero H_c value for the Cu atom, considering the high values for the others atoms in this series. Furthermore, except for Zn, they all present negative H_c values. In both these clusters is observed that the major contribution to the spin density at iron nuclei arises from localized electrons, which contribute with negative values.

For these clusters the N atom again is an acceptor for electrons, suffering an inflow of about one half of that obtained for the clusters centred at FeI sites, furnished also by the FeII sites. This result confirms its character of receptor for electrons in this matrix. Unlikely from before, Q_N decreases slightly through this series. With a lower electronic population related to the other results, the N sites now present a little higher μ values, although exhibiting the same kind of magnetic polarization (opposite to the FeII sites).

The first iron neighbors of a FeII site are 4 atoms at FeI sites and 8 atoms at FeII sites, which were treated on an equal footing. Table 2 shows that these neighbors are almost insensitive to the occupancy of the central site, with respect to the electronic population. The μ_{NN} value is practically independent of that, except for the Cr atom, which caused a reversed μ orientation of the first iron neighbors. The μ_c contribution is also vanishingly small.

For the second shell of neighbors is observed the same behavior of the first neighborhood, i. e., an insensitivity to the occupancy of the central site in this type of cluster.

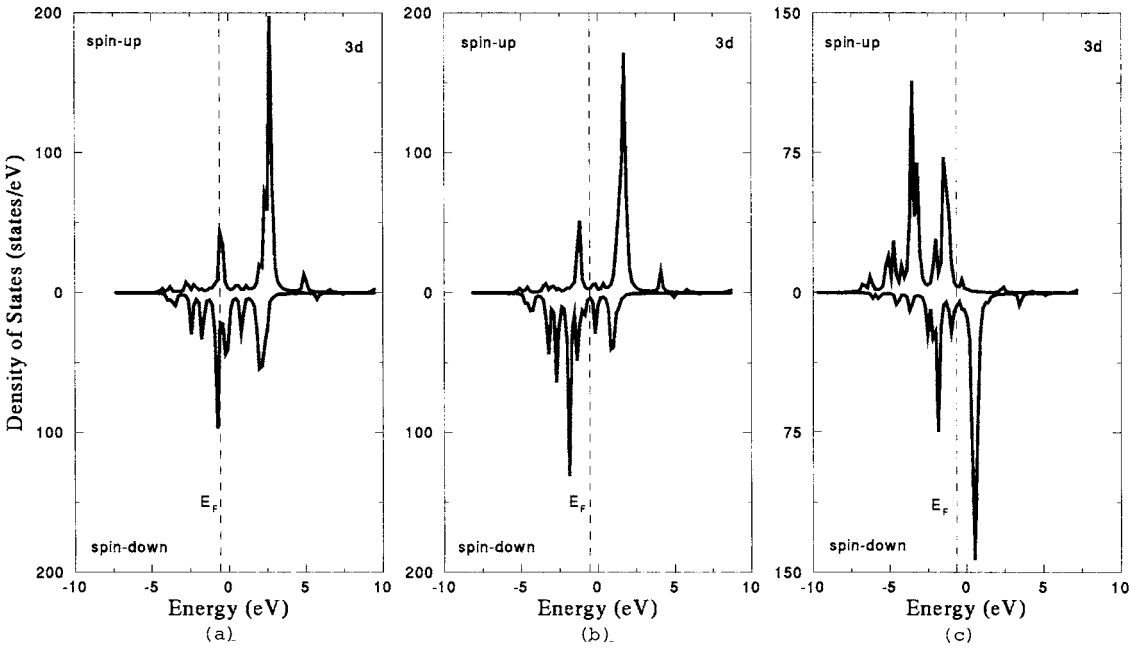

Figure 3. 3d PDOS for the Cr (a) and Mn (b) impurities at the FeI site; (c) the pure host PDOS.

The partial density of states (PDOS) are shown in figs. 2-7, for both FeI and FeII central sites. They are broadened by a Lorentzian profile, according to the energy precision of the calculations, in order to obtain a continuum. No significant change of structure was observed throughout this series for the conduction band, which have similar shapes to that of pure $\gamma' - Fe_4N$. The host 3d PDOS is shown in Fig. 3c, for comparison. The structure of t_{2g}-like peaks of the host is drastically reduced, for those impurities atoms at the left of iron in the periodic table. This reflects the opposite orientation of their magnetic moments, relative to the pure host.

Figs. 2a-2c show the $3d$ PDOS at FeI site for Sc, Ti and V. No significant change of structure was observed throughout this series. In these diagrams one can see how the spin-down states are being increasingly filled up by the incoming d electrons, thus increasing the μ value, which is negative. For the Cr atom (Fig. 3a), the additional d electron is almost entirely located in the spin-down band, which increases the μ value. The $3d$ PDOS shows a resonant peak just on the Fermi energy (E_F), in the spin-down band, besides a very pronounced peak for spin-up electrons. Nevertheless, the incoming d electron of Mn prefers the spin-down states, increasing again the local moment, which in turn achieves its maximum. Fig. 3b shows for the Mn atom two e_g-like peaks just above E_F, for the spin-down virtual bound states, and a very pronounced peak for spin-up states. For the pure host, Fig. 3c displays a full filled 3d band for spin-up states. This reverses the sign of the local moment. The additional d electron of Co is partially located in the spin-down band and thereby decreasing μ (Fig. 4a). For the Ni atom, the next d electron occupies the spin-down band, decreasing μ again (Fig. 4b). Note the large peak just over E_F for Ni, in the spin-down band, where is the only possible occupation for the next d electron of Cu. One feature depicted from these diagrams is the accumulation of the d states near the Fermi surface, leaving empty the bottom of the d band.

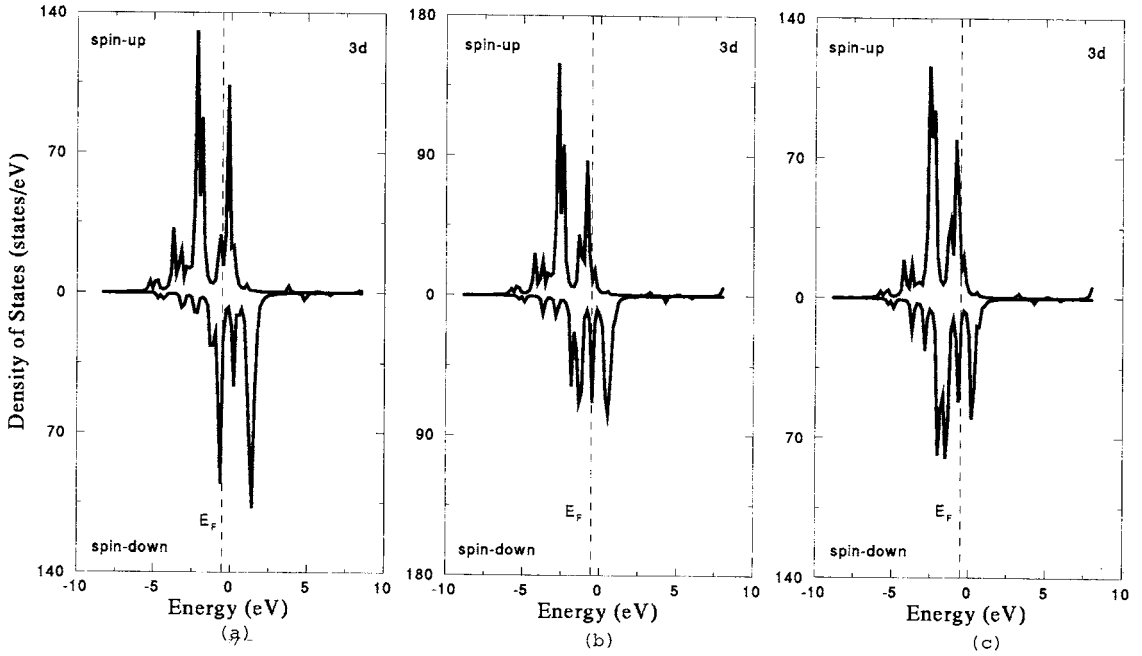

Figure 4. 3d PDOS for the Co (a), Ni (b) and Cu (c) impurities at the FeI site.

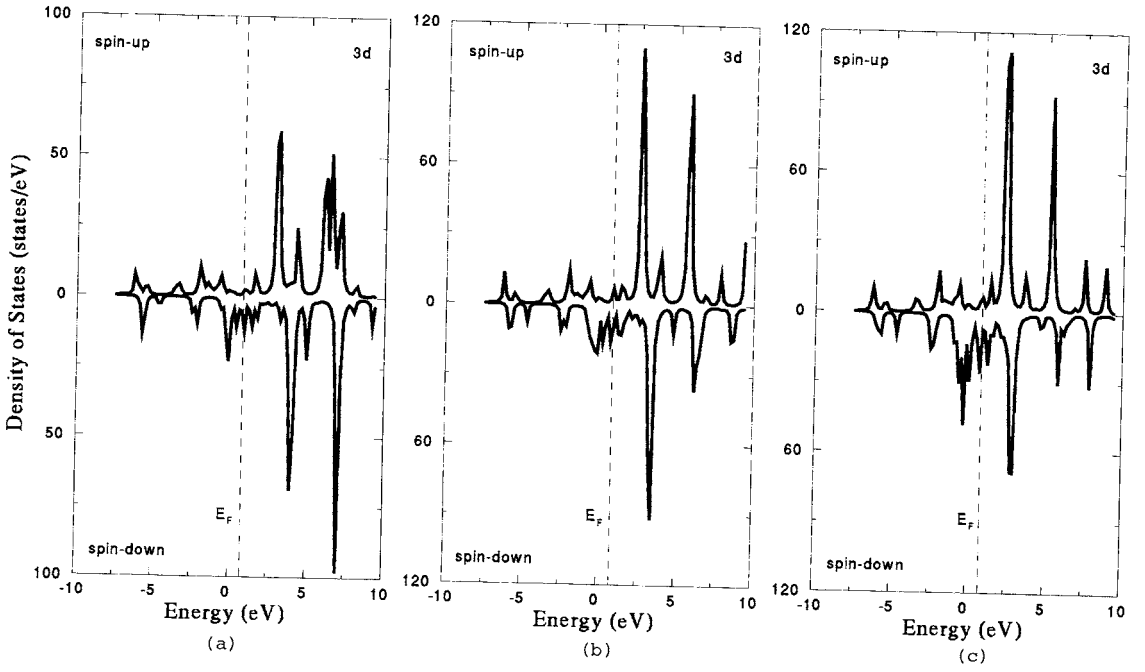

Figure 5. 3d PDOS for the Sc (a), Ti (b) and V (c) impurities at the FeII site.

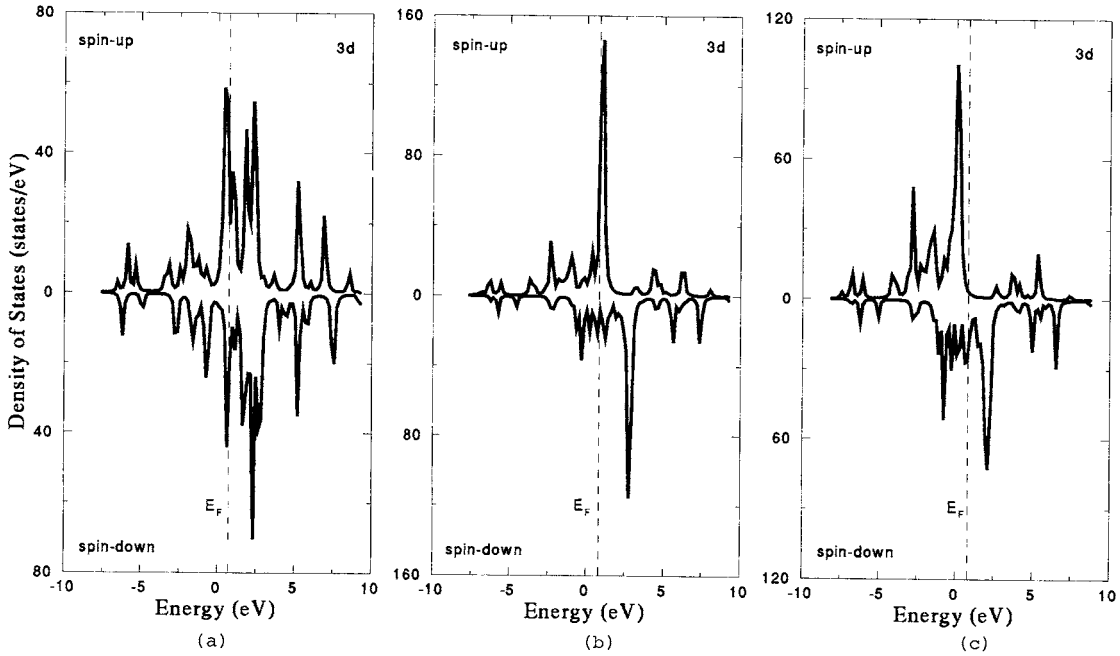

Figure 6. 3d PDOS for the Cr (a), Mn (b) and Fe (c) at the FeII site.

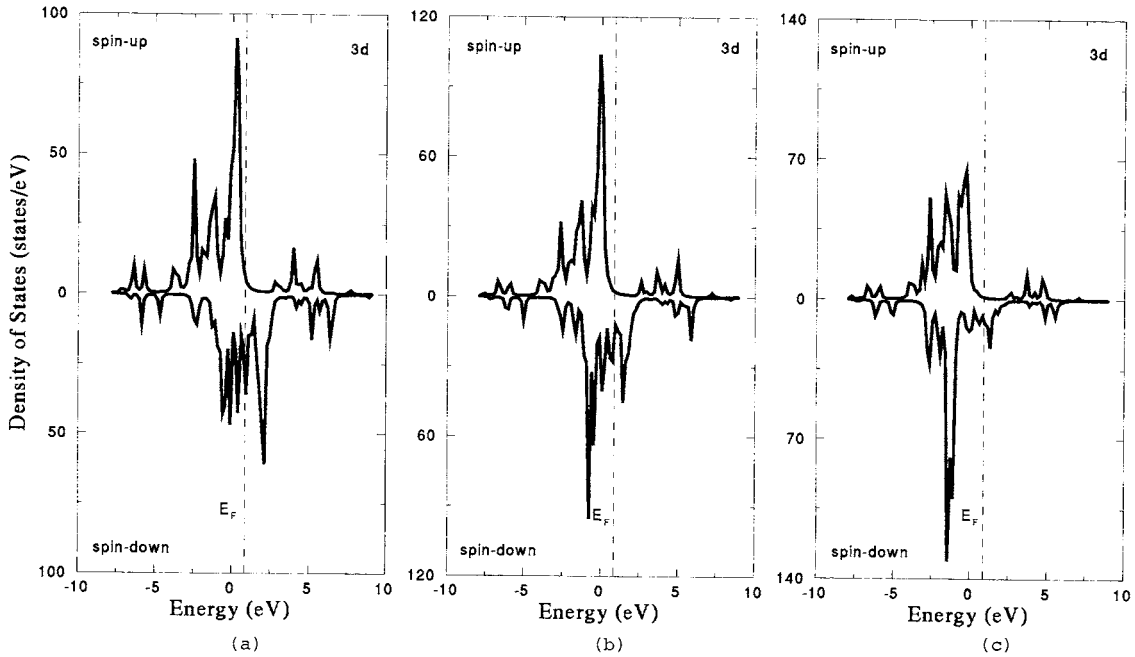

Figure 7. 3d PDOS for the Co (a), Ni (b) and Cu (c) impurities at the FeII site.

The PDOS for the impurities at the FeII sites are shown in Figs. 5-7. A remarkable feature in these diagrams is the broader d bands. Fig. 5 shows an intensive structure of e_g-like peaks for the virtual bond states, whose weighs are shifting to lower energies from Sc to V, whereas the spin-down band is being increasingly occupied. Observe in Fig. 6a how states accumulate at the Fermi surface for the Cr atom, where $\vec{\mu}$ reverses its sign. For the Mn atom, Fig. 6b displays a more localized character (in energy) for the $3d$ band, with a proeminent peak at E_F. For the pure host one can observe in Fig. 6c that the spin-up d states are almost full filled, with the weight of this PDOS close to the Fermi surface. The additional d electron of Co is partially located in the spin-up band, while the spin-down d states becomes more distributed in energy, thus decreasing the local moment. One can observe also that the spin-up states are almost fully occupied since the Mn atom (Fig. 6b). Thus, the next d electron of Cu enters in the spin-down band, which in turn decreases the magnetic moment. It is worth to mention that, in this site, there is a small contribution from d electrons to the magnetic moment of Zn, unlike at FeI site, where it arises totally from the conduction electrons.

The electronic structure of magnetic impurities in Pd was investigated by Zeller, taking into account the perturbations of the electronic potential for up to 1060 surrounding Pd atoms, calculated self-consistently by the multiple-scattering KKR Green-function method. The magnetization cloud on the Pd atoms contained up to 200 host atoms, according to the results of neutron scattering measurements. The calculations show rather extended magnetic polarization clouds around the impurities in that host, due to the presence of the giants moments in Pd atoms (it is about 10 for Fe and Co impurities). The calculations indicate that the clouds are mainly determined by the strong exchange enhancement in Pd atoms, and no Friedel-type oscillatory behaviour was found within the range of 1061 atoms around the impurities.

In the present calculations, considering the relatively small values for the local magnetic moments, the magnetic polarization of the surrounding iron atoms have a small effect. In fact there is no significative changes in the electronic population of the surrounding iron atoms and the changes in the local moments of the conduction band are even smaller. Actually, in view of the not too large values for the local moments in this matrix, one should expect a small magnetic polarization cloud in this case, which could include only a few shell of neighbors. No exchange enhancement kind of mechanism is expected in this case.

III. Summary

Self-consistent spin-polarized cluster calculations were performed with the first-principles DV method in the LSD approximation, to investigate the formation of localized magnetic states and local magnetic properties of $3d$ impurities in the matrix of the ferromagnetic iron nitride $\gamma' - Fe_4N$. For the series of the iron group with Sc, Ti, V, Cr, Mn, Co, Ni, Cu and Zn as impurities atoms at the center of the clusters, the calculations indicate that, at FeI sites, all of these atoms are magnetic impurities. However, at FeII sites only the Cu atom is completely depolarized exhibiting null value for both the local magnetic moment and H_c. At FeI sites is observed the highest μ values for Mn, Cr and Co, whereas at FeII sites these belong to the Mn, V and Co atoms. At both iron sites the Mn atom has the largest H_c value. For the two kinds of occupations, the N atom still is maintaining its character of acceptor for electrons.

Acknowledgement

This work was supported by Financiadora de Estudos e Projetos (Finep) and Conselho Nacional de Desenvolvimento e Pesquisa Tecnológico (CNPq), Brazilian agencies.

References

[1] B. C. Frazer, Phys. Rev. **112**, 751 (1958).

[2] C. Lo, S. V. Krishnawamy, R. Messier, R. P. M. Rao and L. N. Mulay, J. Vac. Sci. Technol. **18**, 2 (1981).

[3] C. A. Kuhnen, R. S. de Figueiredo, V. Drago and E. Z. da Silva, J. Magn. & Magn. Mater. **111**, 95 (1992).

[4] Wei Zhou, Li-jia Qu and Qi-ming Zhang, Phys. Rev. **B40**, 6393 (1989).

[5] A. Sakuma, J. Phys. Soc. Jap. **60**, 6, 2007 (1991).

[6] C. Paduani and J. C. Krause, J. Magn. & Magn. Mater. **138**, 109 (1992).

[7] C. Cordier-Robert and J. Foct, Eur. J. Solid State Inorg. Chem. **29**, 39 (1992).

[8] P. Rochegude and J. Foct, Annales de Chimie France, **8** , 533 (1983).

[9] G. Shirane, J. W. Takei and S. L. Ruby, Phys. Rev., **126**, 49 (1962).

[10] B. Delley, D. E. Ellis and A. J. Freeman, J. Magn. & Magn. Mater. **30**, 71 (1982).

[11] D. Guenzburger and D. E. Ellis, J. Magn. & Magn. Mater. **59**, 139 (1986).

[12] H. Chacham, E. G. da Silva, D. Guenzburger and D. E. Ellis, Phys. Rev. B **35**, 4, 1602 (1985).

[13] B. V. Reddy, S. N. Khanna and B. I. Dunlap, Phys. Rev. Lett. **70**, 3323 (1993).

[14] Z. Q. Li and B. L. Gu, Phys. Rev. B **47**, 13611 (1993).

[15] . D. Ellis, Inter. J. Quantum Chem. **2S**, 35 (1968); D. E. Ellis and G. S. Painter, Phys. Rev. **B2** 2887 (1970), G. S. Painter and D. E. Ellis, Phys. Rev. B1, **12**, 4747 (1970); A. Rosen, D. E. Ellis, H. Adachi and F. W. Averill, J. Chem. Phys. **65**, 9, 3629 (1976).

[16] F. W. Averill and D. E. Ellis, J. Chem. Phys. **59** 12, 3412 (1973).

[17] U. von Barth and L. Hedin, J. Phys. **C5**, 1629 (1972).

[18] C. Umrigar and D. E. Ellis, Phys. Rev. **B21**, 2 (1980).

[19] D. E. Ellis, G. A. Benesh and E. Byron, Phys. Rev. **B20**, 1198 (1979).

[20] R. Zeller : Modelling Simul. Mater. Sci. Eng. **1**, 553 (1993).